RSC Advances

PAPER

View Article Online
View Journal | View Issue

Cite this: *RSC Adv.*, 2017, **7**, 30839

Controlled hydrogen generation using interaction of artificial seawater with aluminum plates activated by liquid Ga–In alloy

Jinrong Lu,[a] Wenbo Yu,[b] Sicong Tan,[a] Lei Wang,[a] Xiaohu Yang[a] and Jing Liu*[ac]

Received 14th February 2017
Accepted 8th June 2017

DOI: 10.1039/c7ra01839h

rsc.li/rsc-advances

Recent studies have disclosed that liquid metal (Ga–In alloy) can be applied to activate aluminum in electrolytes to generate hydrogen at room temperature. To present a close to reality experimental demonstration of this method and to realize a continuous reaction between an Al plate and seawater, the liquid metal GaIn10 alloy is adopted to directly erode the surface of the Al plate. Then the eroded Al plate is immersed into NaCl solution (simulated seawater) to produce hydrogen. The results indicate that the existence of gallium can accelerate the average H_2 production rate. In addition, the average hydrogen generation rate increased from 3×10^{-5} L s^{-1} to 4.5×10^{-4} L s^{-1} as the temperature rose from 20 °C to 80 °C when the corrosion area of the Al plates was 1×10^{-4} m^2. However, the H_2 production first increased and then decreased with the increase of NaCl concentration. The average hydrogen generation effectiveness is 0.71 L g^{-1} in the aluminum–water reaction in 5% NaCl solution at 20 °C within 20 min. Over the experimental process, the capability of producing hydrogen has a linear relationship with the corrosion area on the surface of the Al plates corroded by the liquid metal. This work suggests good prospects in the future practice of large-scale hydrogen generation using Al and seawater as reaction sources.

1. Introduction

Hydrogen is regarded as the next generation clean energy.[1] Traditional hydrogen production strategies are to decompose water using solar energy or electrolysis.[2–7] But the high energy consumption and poor controllability in the decomposition process often lead to serious technical bottlenecks for large scale utilization of hydrogen. In addition, the flammable and explosive characteristics also increase the difficulty of H_2 storage and transportation.[8,9] Hence, it is critical to find and develop a highly convenient method of H_2 production for the coming increasing use.

As one of the critical energy storage materials, Al possesses many advantages, such as low cost, high energy density and large reserves.[10] In addition, the on-site and instant hydrogen generation using Al or its alloys and water can ensure a high level of safety.[11–19] For example, Kazuhiko *et al.*[12] showed that Al could continuously react with water under low vacuum at temperatures above 40 °C. Generally, the powders of Al or Al alloys are used as raw materials to enhance the efficiency.[11–14] The Al powders are often milled in vacuum or inert gases to reduce the particles size.[15] However, the oxidation of Al can form a dense protective alumina film on its surface. This protective surface restrains the Al–water reaction and seriously limits the further development of this technology.[16–20] Therefore, an acid or alkali is often introduced into the solution to promote the modified Al–water reaction. But the use of strong acid or alkali for large-scale hydrogen production would have adverse effects.[16–18] Recent studies reveal that mixing Al and liquid metal in electrolyte can trigger the direct generation of hydrogen, which differs from the traditional strategy of the Al–water reaction for hydrogen production.[19,20] The oxide layer on Al foil can be easily destroyed by a liquid metal (such as Ga or its alloy) at room temperature.[20] However, the liquid alloy needs to be sealed to avoid its contact with water in case of explosion.

As is known, seawater covers most of the earth's surface. It is considered as a potential reservoir for producing hydrogen gas.[21] Chen *et al.*[22] revealed that a mixture of Al, CaO and salt powder could be used as the starting material to prepare Al-based materials by the mechanical ball-milling method for hydrogen generation. This has proven that hydrogen gas can typically be generated through inserting the treated Al alloys in NaCl solution (the main content of sea water). However, the starting materials are somewhat complex and the procedures significantly increase the cost. Based on the above discussion, to reduce the cost of H_2 generation and guarantee security, we

[a]*Beijing Key Lab of CryoBiomedical Engineering, Key Lab of Cryogenics, Technical Institute of Physics and Chemistry, Chinese Academy of Sciences, Beijing 100190, China. E-mail: jliu@mail.ipc.ac.cn; Fax: +86-010-82543767; Tel: +86-010-82543765*
[b]*School of Material Science and Engineering, Tsinghua University, Beijing 100084, China*
[c]*Department of Biomedical Engineering, School of Medicine, Tsinghua University, Beijing 100084, China*

aim to establish a direct way of producing hydrogen with solid Al plate treated by liquid metal and NaCl solution (simulated seawater). Furthermore, the influence of the NaCl concentration and temperature on the hydrogen generation rate will be investigated.

2. Experimental section

6061 aluminum-alloy plates, liquid metal GaIn10 (10 wt% In) and NaCl aqueous solution were used as the raw materials in this work. The experimental process is given in Fig. 1. The Al plates with dimensions of 10 mm × 10 mm × 3 mm were polished using diamond paste. Then the surface of the Al plate was ultrasonically cleaned in ethanol for 20 min. To destroy the Al_2O_3 film, the liquid metal GaIn10 was kept on the surface of the Al plate for 10–30 min. After that, the liquid metal was recycled in a glass flask by spraying alcohol on the surface of the Al, as shown in Fig. 1e. Finally, the prepared Al plate was immersed into NaCl solution with different concentrations. Fig. 1f shows that the volume of hydrogen was measured by a flowmeter. When the processed samples with a rough surface were immersed into NaCl solution, a vigorous reaction occurred and large amounts of hydrogen bubbles were observed on the surface of the Al plate. Basically, when the Al plate was immersed into NaCl solution, H_2 was produced almost immediately.

In order to study the dependence of the amount of hydrogen generated on the corrosion area, Al plates of the same size (10 mm × 10 mm × 3 mm) were used. One side of the surface was covered with liquid metal, so the corrosion area of one Al plate is 1×10^{-4} m^2.

Before and after the reaction, the surface of the Al plate was observed using scanning electron microscopy (SEM) (S-4300, Hitachi, Ltd., Japan). The elemental distribution in the corrosion area was measured using energy dispersive spectrometry (EDS) (6853-H, HORIBA, Ltd., Japan). Furthermore, atomic force microscopy (AFM) (ICON2-SYS, Bruker Nano Inc.) was used to detect the surface roughness of the Al plates. Finally, the phase compositions of the samples were analyzed by X-ray diffraction analysis with a D/Max 2200 PC diffractometer (CuKα, Japan).

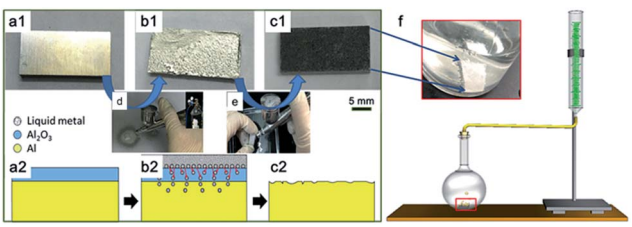

Fig. 1 (a1), (b1) and (c1) The pre-processing of Al plate surface modified by liquid metal; (a2), (b2) and (c2) the schematic diagrams representing (a1), (b1) and (c1) processes, respectively; (d) the coating process *via* spray painting; (e) the recycling process of liquid metal; (f) illustration of the hydrogen generation process. The inset inside the flask indicates the reaction process and the hydrogen gas (bubbles) generates rapidly on the Al surface.

3. Results and discussion

3.1 Hydrogen generation

Fig. 2 shows the morphologies of the Al plates under different conditions, including the Al plate in water (Fig. 2a) and in NaCl solution (Fig. 2b), the Al plate processed by liquid metal in water (Fig. 2c) and in NaCl solution (Fig. 2d) respectively. Fig. 2a and b reveal that no bubbles were produced when the untreated Al plate was immersed in water and in NaCl solution. In contrast, when the Al plate treated using liquid metal was immersed in water (Fig. 2c) and NaCl solution (Fig. 2d), bubbles were generated on the Al plate surface, and an especially vigorous reaction occurred in Fig. 2d.

These results suggest that GaIn10 plays the role of catalyst and that the existence of NaCl can accelerate the H_2 production rate. Furthermore, they demonstrate that the Al plate eroded by GaIn10 can be used for H_2 generation at room temperature in atmosphere. In addition, this method is simpler and safer to run than those performed using Al powder and/or under high pressure and high temperature.[12–18]

Fig. 3 presents the variation of the generated H_2 content with time and temperature under different concentrations of NaCl solution. Due to the large differences of the average H_2 production rate in different conditions, the H_2 production time is taken as the ordinate. Fig. 3a shows that the H_2 production rate in NaCl solution is obviously higher than that in water. The

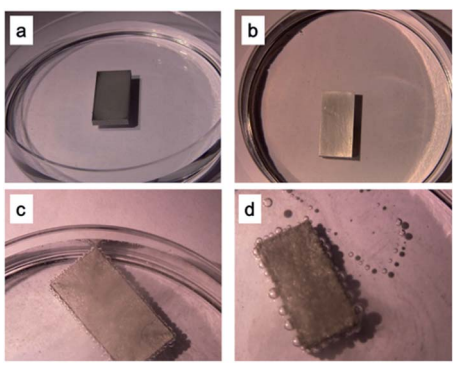

Fig. 2 Hydrogen generation modes under 4 different conditions: (a) and (b) Al plate in water and in 5% NaCl solution; (c) and (d) the Al plate processed with liquid metal in water and in 5% NaCl solution.

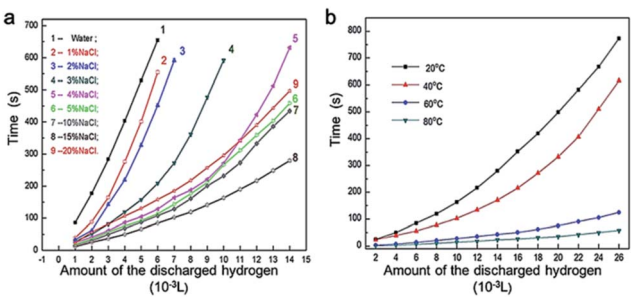

Fig. 3 The relationship between the amount of discharged hydrogen and time: (a) under different concentrations of NaCl solution; (b) under different temperatures.

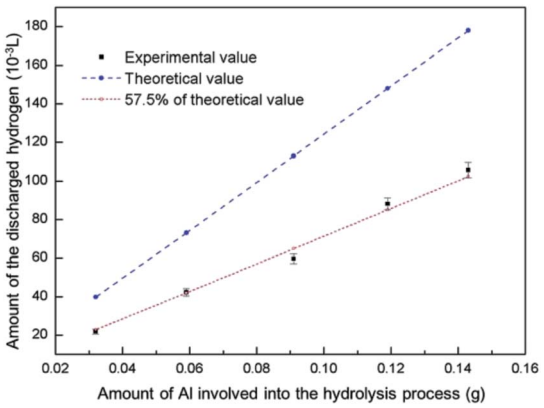

Fig. 4 The relationship between the amount of Al involved into the hydrolysis process and the discharged hydrogen in 5% NaCl solution at 20 °C for 20 min.

average H_2 production rate increased from 1×10^{-5} L s^{-1} to 5×10^{-5} L s^{-1} as the NaCl solution concentration increased from 0 to 15% at 20 °C when the corrosion area of Al plates is 1×10^{-4} m^2. After that, the average H_2 production rate decreased significantly to 3×10^{-5} L s^{-1} when the concentration increased to 20% as the corrosion area of Al plates is 1×10^{-4} m^2.

Salt can impede the cold fusion of Al particles and thus reduced their size.[23] In addition, the fresh surfaces of the Al particles were covered by salt, which prevented the formation of the oxidation. As a result, the effective contact between the water and small Al particles with huge specific areas remarkably enhanced the reaction kinetics.[23,24] In terms of the influence of temperature, Fig. 3b reveals that the average H_2 production rate increased continuously from 3×10^{-5} L s^{-1} to 4.5×10^{-4} L s^{-1} when the temperature increased from 20 °C to 80 °C in 5% NaCl solution as the corrosion area of Al plates is 1×10^{-4} m^2. This strongly suggests that the hydrogen generation rate depends crucially on the initial temperature of the water. Therefore, it was feasible to employ the heat produced during the process of exothermic reaction between the Al and water.[25]

Based on Fig. 3b, Arrhenius plot ($\ln r$ *vs.* T^{-1}) can be obtained and the slope is used to calculate the activation energy (Ea) by using the following equation:[26]

$$E_a = -R \frac{d(\ln r)}{d\left(\frac{1}{T}\right)} \quad (1)$$

where R is the gas constant, r is the H_2 production rate, and T is the temperature.

It has been calculated that the activation energy (E_a) of the hydrogen generation is 3.96×10^4 J mol^{-1} in 5% NaCl solution.

After the erosion of the liquid metal (the corrosion area of one Al plate is 1×10^{-4} m^2), the weight of the Al plate decreased from 1.601 g to 1.588 g, and the Al plate's weight decreased to 1.556 g after the H_2 generation with 5% NaCl solution at 20 °C for 20 min.

Finally, 0.032 g of Al is consumed during this H_2 generation and the amount of discharged hydrogen is 2.18×10^{-2} L.

Fig. 4 depicts the dependence of the amount of discharged hydrogen on different amount of Al involved into the hydrolysis process in 5% NaCl solution at 20 °C for 20 min. It indicates that the amount of discharged H_2 is proportional to the amount of Al. In reference to the following equation,[27]

$$2Al + 6H_2O \rightarrow 2Al(OH)_3 + 3H_2 \quad (2)$$

under ideal conditions, 5.97×10^{-2} L hydrogen gas can be generated by 0.091 g Al, and 1.06×10^{-1} L hydrogen gas can be generated by 0.143 g Al, so the average hydrogen generation effectiveness is 0.71 L g^{-1}. Compared with the experimental value, the average production efficiency is 57.5%, and the experimental values are lower than the theoretical values, as shown in Fig. 4b.

For comparison, some studies on the reaction of aluminum or its alloys with water for H_2 generation are summarized. It is found that, the H_2 conversion yields in Table 1 are mostly greater than the efficiency in our study. Especially, the conversion yield using Al alloys with different compositions as raw materials using melting at 82 °C could reach 100%.[17] However, the high efficiency of these methods was based on the premise of the complex preparation processes such as ball milling[14] or melting,[17] which lead to a large amount of cost of human and material resources. What is more, all the raw materials are powers, even super fine powder,[23] and some of the chemical reaction needs a alkaline environment to produce hydrogen.[16,20]

In contrast, due to the low-cost of the Al plate and seawater used in this study and the simple preparation technology as taken, the current result is suitable for various occasions.

Fig. 5 presents the influence of the GaIn10 infiltrated depth in the Al plate on the amount of discharged hydrogen. As shown in Fig. 5a, the infiltrated depth of GaIn10 into the Al plate increases linearly from 18.2 μm to 26.9 μm within 10–20 min at 20 °C, which is in accordance with the macroscopic diffusion rules. Subsequently, the average H_2 production rate in 5 wt% NaCl solution at 20 °C was measured (Fig. 5b). The average H_2

Table 1 Studies on hydrogen production from Al (or Al alloys) with water

Raw materials	Treatment	Temperature (°C)	H_2 conversion yield	References
Al–Bi (hydride or solid salt)	Ball milling for 5 h	25	93.4%	14
Al–Si alloys	Alkaline solution (NaOH, KOH, $Ca(OH)_2$)	25–75	76%	16
Al alloys with different compositions	Melting	82	100%	17
Al–Si alloys	Alkaline solution (NaOH) and atomization of $NaBH_4$	75	94%	20
Al–Ga–In–Sn–Zn powders	The powder particle sizes are less than 250 nm	21 or 60	50–55% or 80–85%	23

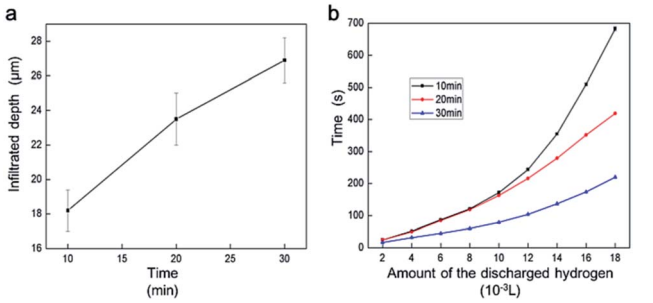

Fig. 5 Influence of the infiltrated depth on the amount of discharged hydrogen: (a) relationship between the infiltrated depth and time; (b) relationship between the amount of discharged hydrogen and time at different infiltration times.

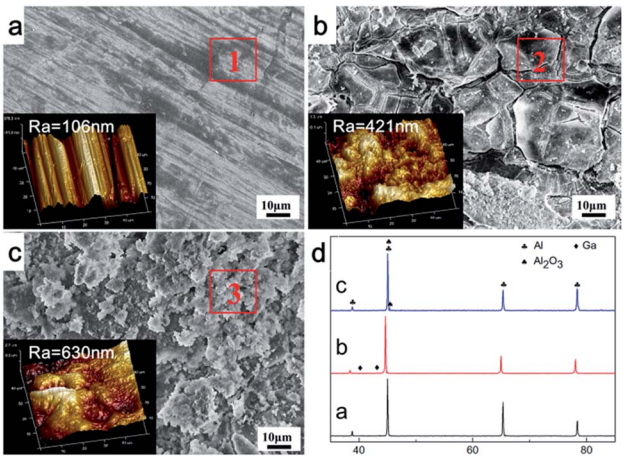

Fig. 6 SEM images and the corresponding AFM images of Al plate surfaces: (a) pure Al plate; (b) Al plate corroded by liquid metal for 10 min at 20 °C; (c) Al plate after H_2 production in 5% NaCl solution at 20 °C for 20 min; (d) XRD patterns of the three Al plate surfaces.

production rates are extracted as 2×10^{-5} L s^{-1} and 8×10^{-5} L s^{-1} in respect to the GaIn10 treatment time of 10 min and 30 min when the corrosion area of Al plates is 1×10^{-4} m^2, respectively.

Liquid metal is not only rather effective in removing the oxidation layer but also enables the Al–water reaction by transporting the Al in alloys to reaction sites.[28,29] When the liquid metal is kept on the surface of the Al plate, Ga atoms can infiltrate into the grain boundaries of polycrystalline Al_2O_3. This can initiate intergranular failure in the Al_2O_3.[30–32] Thus, when the liquid metal is recycled, the Al_2O_3 can be easily removed from the surface of the Al plate. Finally, the weight of the Al plate decrease, as shown in Fig. 4b. Moreover, the liquid metal continues to infiltrate into the Al plate and lowers the surface energy of the Al.[30] With the increase of the infiltrated depth, more fine Al particles appear. As small size particles can enhance the reaction kinetics,[23] the surface activity of the Al increase and the average H_2 production rate is improved, as shown in Fig. 5b.

3.2 Topographies and content analysis

Fig. 6 presents the typical SEM micrographs of the plate surfaces combined with the corresponding AFM images in different conditions. For the untreated Al plate, Fig. 6a shows that the surface was smooth and intact. For the treated Al plate, Fig. 6b indicates that huge extensive cracks formed on the surface of the Al plate. The cracks were mainly located and propagated along the Al grain boundaries. After the H_2 generation process, the cracks on the surface of the Al plate disappeared. Instead, snowflake lamella structures appeared, as shown in Fig. 6c. Furthermore, the average roughness (R_a) detected by AFM on the three regions are 106 nm, 421 nm and 630 nm, respectively. These results further confirmed that liquid metal GaIn10 could break up the Al_2O_3 layer on the Al plate surface and favored the penetration of H_2O along the Al grain boundaries.

Table 2 summarized the elemental composition of the three Al plates determined with EDS. The detected areas are marked as rectangles in Fig. 6. After the erosion of GaIn10 on the Al plate, 3.9 wt% of Ga and negligible amounts of In were detected, as revealed in Table 1 and the XRD analyses in Fig. 6d. This is in accordance with the reported results: Ga is highly soluble in solid Al while In is not.[33,34] Here, it should be pointed out that the oxygen was eliminated for an approximate assumption in the EDS analysis, because the existence of oxygen could cause inaccurate measurement of Ga and In. After 20 minutes of H_2 production, the Ga almost disappeared. The corresponding XRD diffraction patterns of the three Al plates reveal that Al_2O_3 and Al peaks can be observed in Fig. 6a and d(c), but not in Fig. 6c.

It has been reported that Ga atoms can incorporate into the Al lattice,[35] which accounts for the absence of diffraction peaks of Ga or its compounds in the reaction products between the Al and liquid metal. As Ga atoms penetrated into the Al lattice,[36,37] the diffraction peaks of Al in Fig. 6d(b) obviously shifted to smaller diffraction angles in comparison with Fig. 6d(a) and d(c).

Fig. 7 shows the elemental distribution obtained from mapping analyses with EDS in the final reaction products after H_2 production. The weight percentage of different elements is summarized in Table 3. Na and Cl are found due to the NaCl solution. According to the reference,[28] O should be from the reaction products of $Al(OH)_3$. As the H_2 production reaction happened at room temperature, it was impossible to form Al–Ga alloys.[34] It can be estimated that Ga functions as a catalyst during H_2 production. Ga atoms can incorporate into the Al lattice,[35] as also shown in Fig. 6d. When the liquid metal is sprayed on the Al plate surface, liquid Ga penetrates into the Al

Table 2 EDS analyses on different regions marked in Fig. 6 (wt%)

	Al	Mg	Ga	In
1	98.7	1.3	0	0
2	94.6	0.9	3.9	0.8
3	98.2	0.7	0.8	0.3

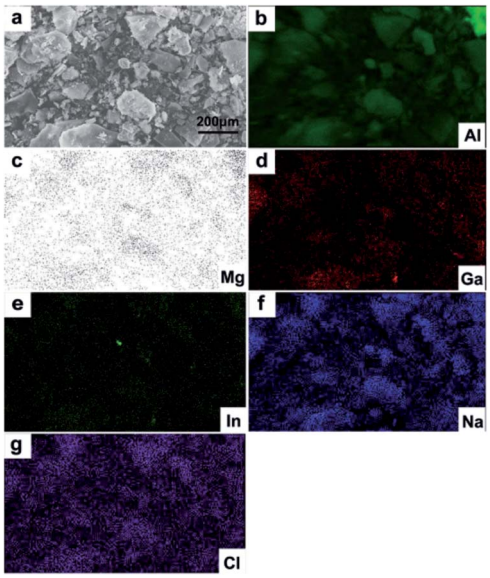

Fig. 7 Elemental distribution of the reaction products in hydrogen production: (a) SEM images of the reaction products; (b–g) distribution of different elements – Al, Mg, Ga, In, Na and Cl.

Table 3 EDS analyses on different elements marked in Fig. 7

Element	Al	Mg	Ga	In	Na	Cl
Wt%	80.98	0.97	3.15	0.59	4.31	10

plate along the Al grain boundaries. This results in a substantial loss of cohesion.[38–40] As Ga penetrated into Al crystallites and destroyed the Al oxide film, the outermost layer of the Al plate cracked and formed tiny cracks, as shown in Fig. 6b. Finally, the reaction between Al and water can occur at room temperature once the Al surface is not blocked by oxide film.[41] Furthermore, it has been reported that the H_2 production rate between Al and water closely depends on the Al powder particle size, and powder with smaller particle sizes can offer a higher reaction rate because of the larger specific surface value.[42] After being corroded, the surface layer of the Al plate is covered by tiny cracks and divided into small parts, which is similar to the Al particles shown in Fig. 6 in our study.

4. Conclusions

In summary, a feasible method of producing hydrogen at room temperature through the direct reaction between GaIn alloy corroded Al plate and sodium chloride (NaCl) solution was successfully demonstrated. The main advantage of this method lies in its high reliability and low cost. Firstly, the average H_2 production rate increased from 1×10^{-5} L s^{-1} to 5×10^{-5} L s^{-1} when increasing the NaCl solution concentration from 0 to 15%, then decreased to 3×10^{-5} L s^{-1} at 20 NaCl solution as the corrosion area of Al plates is 1×10^{-4} m^2. Secondly, with increase of the temperature from 20 °C to 80 °C, the average H_2 production rate increased from 3×10^{-5} L s^{-1} to 4.5×10^{-4} L s^{-1} as the corrosion area of Al plates is 1×10^{-4} m^2. Thirdly, the amount of hydrogen generated was proportional to the corrosion area on the surface of the Al plates. The average hydrogen generation effectiveness was 0.71 L g^{-1} in 5% NaCl solution at 20 °C within 20 min, and the average efficiency of the hydrogen evolution was about 57.5%. Further research revealed that the outermost layer of Al plate cracked and formed tiny cracks due to penetration of the liquid Ga into the Al plate along the Al grain boundaries. This favored the reaction between Al and water. During the reaction processes, the liquid metal served as a catalyst and could be collected for repeated use. Future research will be aimed at improving the efficiency of hydrogen production.

Acknowledgements

This work is partially supported by the Beijing Municipal Science and Technology Project (Grant No. Z151100003715002) and the China Postdoctoral Science Foundation (Grant No. 2016M590137). Great thanks are given to Dr Li-ting Yi, Mr Yu-jie Ding in the lab for their help in the experiments.

References

1 A. Bauen, *J. Power Sources*, 2006, **157**, 893.
2 C. Wu, *Progr. Chem.*, 2005, **17**, 423.
3 W. Li, X. F. Gao, D. H. Xiong, *et al.*, *Chem. Sci.*, 2017, **8**, 2952.
4 W. Li, X. Gao, X. Wang, *et al.*, *J. Power Sources*, 2016, **330**, 156.
5 W. Li, D. Xiong, X. Gao, *et al.*, *Catal. Today*, 2017, **287**, 122.
6 W. Li, X. Wang, D. Xiong, *et al.*, *Int. J. Hydrogen Energy*, 2016, **41**, 9344.
7 X. Wang, W. Li, D. Xiong, *et al.*, *Adv. Funct. Mater.*, 2016, **26**, 4067.
8 J. Turner, G. Sverdrup, M. K. Mann, *et al.*, *Int. J. Hydrogen Energy*, 2008, **32**, 379.
9 M. Ball and M. Wietschel, *Int. J. Hydrogen Energy*, 2009, **34**, 615.
10 H. Z. Wang, D. Y. C. Leung, M. K. H. Leung, *et al.*, *Renewable Sustainable Energy Rev.*, 2009, **13**, 845.
11 Z. Y. Deng, J. M. F. Ferreira, Y. Tanaka, *et al.*, *J. Am. Ceram. Soc.*, 2007, **90**, 1521.
12 M. Kazuhiko, T. Kentaro, L. Daling, *et al.*, *Nature*, 2006, **440**, 295.
13 Z. Y. Deng, Y. F. Liu, Y. Tanaka, *et al.*, *J. Am. Ceram. Soc.*, 2005, **88**, 2975.
14 M. Q. Fan, L. X. Sun and F. Xu, *J. Alloys Compd.*, 2008, **460**, 125.
15 W. Z. Gai, W. H. Liu, Z. Y. Deng, *et al.*, *Int. J. Hydrogen Energy*, 2012, **37**, 13132.
16 L. Soler, J. Macanás, M. Muñoz, *et al.*, *J. Power Sources*, 2007, **169**, 114.
17 O. V. Kravchenko, K. N. Semenenko, B. M. Bulychev, *et al.*, *J. Alloys Compd.*, 2005, **397**, 58.
18 L. Soler, A. M. Candela, J. Macanás, *et al.*, *J. Power Sources*, 2009, **192**, 21.
19 B. Yuan, S. C. Tan and J. Liu, *Int. J. Hydrogen Energy*, 2015, **41**, 1453.

20 L. Soler, J. Macanás, M. Muñoz, *et al.*, *Int. J. Hydrogen Energy*, 2007, **32**, 4702.
21 H. Elderfield and M. J. Greaves, *Nature*, 1982, **296**, 214.
22 X. Chen, Z. Zhao, M. Hao, *et al.*, *J. Power Sources*, 2013, **222**, 188.
23 A. V. Ilyukhina, A. S. Ilyukhin and E. I. Shkolnikov, *Int. J. Hydrogen Energy*, 2012, **37**, 16382.
24 T. Hiraki, M. Takeuchi, M. Hisa, *et al.*, *Mater. Trans.*, 2005, **46**, 1052.
25 K. Mahmoodi and B. Alinejad, *Int. J. Hydrogen Energy*, 2010, **35**, 5227.
26 F. Wang, C. Li, X. Zhang, *et al.*, *J. Catal.*, 2015, **329**, 177.
27 Y. Yavor, S. Goroshin, J. M. Bergthorson, *et al.*, *Int. J. Hydrogen Energy*, 2013, **38**, 14992.
28 E. Czech and T. Troczynski, *Int. J. Hydrogen Energy*, 2010, **35**, 1029.
29 J. T. Ziebarth, J. M. Woodall, R. A. Kramer, *et al.*, *Int. J. Hydrogen Energy*, 2011, **3**, 5271.
30 R. Stumpf and P. J. Feibelman, *Phys. Rev. B: Condens. Matter Mater. Phys.*, 1996, **54**, 5145.
31 D. I. Thomson, V. Heine, M. W. Finnis, *et al.*, *Philos. Mag. Lett.*, 1997, **76**, 281.
32 E. Pereiro-López, W. Ludwig and D. Bellet, *Acta Mater.*, 2004, **52**, 321.
33 H. Okamoto, *J. Phase Equilib. Diffus.*, 2012, **33**, 413.
34 A. V. Ilyukhina, O. V. Kravchenko, B. M. Bulychev, *et al.*, *Int. J. Hydrogen Energy*, 2010, **35**, 1905.
35 M. V. Trenikhin, A. V. Bubnov and A. I. Nizovskii, *Russ. J. Phys. Chem. A*, 2016, **80**, 1110.
36 W. Wang, D. M. Chen and K. Yang, *Int. J. Hydrogen Energy*, 2010, **35**, 12011.
37 S. Fung, X. Xu, Y. Zhao, *et al.*, *J. Appl. Phys.*, 1998, **84**, 2355.
38 C. D. S. Tuck, J. A. Hunter and G. M. Scamans, *J. Electrochem. Soc.*, 1987, **134**, 2970.
39 A. V. Parmuzina and O. V. Kravchenko, *Int. J. Hydrogen Energy*, 2008, **33**, 3073.
40 A. V. Parmuzina, O. V. Kravchenko, B. M. Bulychev, *et al.*, *Russ. Chem. Bull.*, 2009, **58**, 493.
41 M. Rajagopalan, M. A. Bhatia, M. A. Tschopp, *et al.*, *Acta Mater.*, 2014, **73**, 312.
42 S. S. Razavi-Tousi and J. A. Szpunar, *J. Alloys Compd.*, 2016, **679**, 364.